Microperoxidase-8 Associated to CTAB Micelles: A New Catalyst with Peroxidase Activity

Tatiana Prieto,[†] Otaciro R. Nascimento,[‡] Ivarne L. S. Tersariol,[†] Adelaide Faljoni-Alario,[§] and Iseli L. Nantes*[,†]

Centro Interdisciplinar de Investigação Bioquímica (CIIB), Universidade de Mogi das Cruzes (UMC), Mogi das Cruzes, SP, Brazil, Instituto de Física de São Carlos (IFSC), Universidade de São Paulo (USP), São Carlos, São Carlos, SP, Brazil, and Instituto de Química (IQ), Departamento de Bioquímica, Universidade de São Paulo, São Paulo, SP, Brazil

Received: December 12, 2003; In Final Form: May 4, 2004

Literature data have pointed to microperoxidase-8 (MP-8) as an attractive water-soluble model for studying the reaction mechanism of peroxidases because this heme peptide is able to form the same enzyme intermediates during reaction with peroxides. In this work, we have demonstrated that the association of Fe(III)MP-8 with CTAB micelles provides a microenvironment with an alkaline interface and a hydrophobic core that gives special characteristics to the Fe(III)MP-8/peroxide (*tert*-butyl hydroperoxide or hydrogen peroxide) reaction as compared with homogeneous medium. EPR spin-trapping studies using 5,5-dimethyl-1-pyrroline *N*-oxide and computer simulations of the experimental spectra were performed to determine the reaction mechanism. From the analysis of the results, alkoxyl and hydroxyl radicals of *t*-BuOOH and HOOH, respectively, were identified as the initial radicals produced, presumably by homolytic scission of the O−O bond by Fe(III)MP-8/CTAB. The UV−vis spectral changes for Fe(III)MP-8 pointed to the formation of Compound II as the species that exhibits subsequent bleaching. The peculiarity of the CTAB micellar microenvironment allowed circumvention of rapid kinetics, permitting the reaction to be accompanied on the scale of seconds. The K_m and the maximal conversion rate (k_2) of CTAB-bound Fe(III)MP-8 into the corresponding Compound II were determined for the reaction with peroxides in 20 mM CTAB, at pH 7.4 and 9.1. For both substrates, the K_m values increased at pH 9.1 without significant changes in k_2 values, indicating alteration in the affinity of the substrates for CTAB-bound Fe(III)MP-8.

Introduction

Microperoxidase-8 (MP-8) is a heme octapeptide obtained by sequential peptic and tryptic digestion of horse-heart cytochrome *c*. Like cytochrome *c*, this peptide exhibits the heme group covalently attached to two cysteine residues through thioether bonds. It exists in the ferric resting state, retains histidine as a fifth heme iron ligand, but does not retain the methionine residue at the sixth coordination position, this position being occupied, at neutral pH, by a water molecule.[1−3] Because of these structural characteristics, MP-8 is able to convert a wide variety of organic compounds at the expense of hydrogen peroxide in a peroxidase-type chemistry.[4] MP-8 high-valent intermediates have been detected during its reaction with hydrogen peroxide, which makes this heme octapeptide a good model for Compounds 0, I, and II of horseradish peroxidase (HRP).[5,6] Compound 0 has been detected for HRP at low temperature and corresponds to the porphyrin iron-hydroperoxide (PorFe(III)-OOH) species.[5] This species precedes the formation of Compounds I and II, which are well-known high-valent HRP intermediates and were also detected during the reaction of N_α-acetyl microperoxidase-8 with hydrogen peroxide.[6]

It is known that protons in the distal heme active site influence the formation of the catalytic reactive species for both peroxidases and cytochrome P450.[7] In HRP, the distal His42 ligand acts as an acid/base catalyst that favors the deprotonation of the hydroperoxide substrate at the enzyme active site (Compound 0) and the subsequent heterolytic cleavage.[8−10] Therefore, the deprotonation of the hydroperoxide in Compound 0 is a crucial step in the catalytic cycle of peroxidases and cytochrome P450.

Besides peroxidases, cytochrome *c* is also able to catalyze peroxide cleavage both free[11] and associated to vesicles.[12] In both conditions, EPR spin-trapping studies using 5,5-dimethyl-1-pyrroline *N*-oxide (DMPO) revealed that the alkoxyl radical adduct is the initial radical produced, which is compatible with homolytic cleavage of peroxides as the principal route.

Recently, a competitive effect of protons has been demonstrated for the reaction of Fe(III)MP-8 or Mn(III)MP-8 with hydrogen peroxide, suggesting that Compound 0 precedes the formation of a high-valent intermediate of Fe(III)MP-8 or Mn(III)MP-8.[13] In comparison with HRP, MP-8 in aqueous medium does not exhibit a site pocket with a distal basic residue participating in the peroxide deprotonation and favoring the O−O peroxide bond cleavage. These characteristics could somehow be responsible for the low reactivity of MP-8 at low pH. In aqueous medium, alkaline pH leads to deprotonation of the MP-8 bound water, which then either assists concerted hydrogen peroxide deprotonation and coordination of the

* Corresponding author. Phone: +55-11-4798-7103. Fax: +55-11-4798-7102. E-mail: ilnantes@umc.br.
[†] UMC.
[‡] IFSC, USP.
[§] IQ, USP.

10.1021/jp037849x CCC: $27.50
Published on Web 06/23/2004

hydroperoxo group to the metal center or is directly oxidized by hydrogen peroxide to a metal−hydroperoxo MP-8.[13]

Previously, we have characterized changes in the heme and the influence of membrane lipids in the reaction of cytochrome *c* with *tert*-butyl hydroperoxide (*t*-BuOOH). In the course of this reaction, *t*-BuOOH-induced Soret band bleaching was accelerated by several negatively charged liposomes.[12] Comparison with the reaction of Fe(III)MP-8 with peroxides (HOOH and *t*-BuOOH) in the presence of different micelles and liposomes revealed that, in this case, the Soret band bleaching also occurred in a medium-dependent manner (not shown). However, cetyltrimethylammonium bromide (CTAB) micelles had a specific effect on the reaction mechanism, leading the Soret band bleaching to be preceded by a gradual bathochromic shift. In this work, we present a study of the mechanism of reaction between a MP-8/CTAB micelle complex and peroxides. The MP-8/CTAB complex behaves as a lipoenzyme and exhibits interesting redox characteristics that will be discussed herein.

Experimental Section

Chemicals. Microperoxidase-8, *t*-BuOOH, DMPO, and CTAB were obtained from Sigma Chemical Co. (St Louis, MO). DMPO was vacuum-distilled at room temperature twice before use. Hydrogen peroxide was purchased from Aldrich (Milwaukee, WI). The concentration of the dilute HOOH solutions was always checked spectrophotometrically using the molar extinction coefficient at 240 nm, $\epsilon_{240} = 39.4 \pm 0.2\ M^{-1}\ cm^{-1}$.[14] All aqueous solutions were prepared with deionized water (mixed bed of ion exchanger, Millipore) and the pH was measured using a combined glass electrode (Orion Glass pH SURE-FLOW). The reference electrode (ROSS, Model 8102) was filled with Orion Filling Solution (ROSS). The pH meter was calibrated using METREPAK pHydrion standard buffer solutions (Brooklyn, NY).

Preparation of Micellar CTAB Solutions. CTAB micellar solutions were prepared by dissolving CTAB in an appropriate buffer with stirring at 37 °C. The cmc (critical micelle concentration) was determined in the usual fashion from plots of the surface tension vs log [CTAB]. Surface tensions were measured with a Du Nouy tensiometer equipped with a Pt ring.

UV−Vis Kinetic Measurements. Solutions of Fe(III)MP-8 and the corresponding HOOH or *t*-BuOOH solutions were both buffered with either 5 mM sodium phosphate (pH 7.4 and 8.1) or 5 mM sodium carbonate (pH 9.1). For Fe(III)MP-8, concentrations of the oxygen donor, HOOH and *t*-BuOOH, were varied from 0.1 to 1.2 mM. The concentration of Fe(III)MP-8 was 4.25 μM and was verified by using $\epsilon_{397} = 1.57 \times 10^5\ M^{-1}\ cm^{-1}$ for Fe(III)MP-8 at pH 7.0.[1] The concentration of Fe(III)MP-8 in CTAB micelles was calculated using $\epsilon_{400} = 1.13 \times 10^5\ M^{-1}\ cm^{-1}$, determined from a standard curve obtained by determining the spectra of Fe(III)MP-8/CTAB at different heme peptide concentrations. All measurements were performed under pseudo-first-order conditions with at least a 10-fold excess of peroxide with respect to the Fe(III)MP-8 concentration at the temperature of 25 ± 0.3 °C.

Time-resolved spectra were recorded on a Shimadzu Model 1501 MultiSpec (Tokyo, Japan), employing the photodiode array scan mode. The spectral resolution was around 0.5 nm, and the spectra were obtained with a time interval of 1 s. The optical path length was 1 cm for all measurements. The data sets represent the average of three independent measurements. The kinetic data were recorded at 417 nm for Fe(III)MP-8/CTAB, the region of strong absorbance of the Compound II species. The observed conversion rate of Fe(III)MP-8/CTAB into Compound II/CTAB obeys an exponential relationship that could be best fit to the first-order equation

$$P = P_\infty[1 - \exp(-k_{obs}t)] \quad (1)$$

where P and P_∞ are the product concentrations at a given time and at infinite time, respectively, and k_{obs} is the observed first-order rate constant for the conversion of Fe(III)MP-8 into Compound II.

The influence of peroxide concentration on the conversion rate of Fe(III)MP-8 into Compound II obeyed eq 2:

$$k_{obs} = \frac{k_2[ROOH]}{K_{m,app} + [ROOH]} \quad (2)$$

where k_{obs} is the observed conversion rate of Fe(III)MP-8 into Compound II, k_2 is the maximum rate, [ROOH] is the concentration of peroxide, and $K_{m,app}$ is the apparent dynamic or pseudoequilibrium constant for complexation between Fe(III)MP-8/CTAB and peroxides.

$K_{m,app}$ is defined by

$$K_{m,app} = \left(1 + \frac{[H^+]}{K_a}\right)\left(\frac{k_{-1} + k_2}{k_1}\right) \quad (3)$$

EPR Spin-Trapping Experiments. The EPR spectra of DMPO adducts were recorded using a Varian E-109 X-band system under the following conditions: modulation amplitude 0.05 mT, microwave power 20 mW, room temperature, scan time 2 min, scan range 100 G, and receiver gain 1.6×10^4. The sample was transferred into the EPR flat cell under anaerobic conditions and was introduced in the microwave cavity 75 s before the measurements were started. The EPR spectra were simulated using the SiMfonia Bruker program, and the hyperfine parameters and line width were obtained for each paramagnetic species.

Heme Iron EPR Measurements. Direct EPR measurements of Fe(III)MP-8 (100 μM) were obtained in a Bruker ELEXSYS EPR System E-580 under the following conditions: gain 5×10^3, modulation amplitude 1.0 mT, microwave power 4 mW, temperature 11 K, time constant 20.48 ms, and conversion time 81.92 ms. After mixing, solutions were quickly introduced into an EPR quartz tube that was previously cooled in liquid nitrogen. After freezing the sample was introduced into the microwave cavity at low temperature and the EPR measurements were performed.

Results

Figure 1 shows that the association of Fe(III)MP-8 with CTAB micelles led to changes in the UV−vis spectrum compatible with the heme group in a nonpolar microenvironment.[15] Figure 1 shows that the UV−vis spectrum of Fe(III)MP-8 exhibits a bathochromic shift of the Soret band in both ethanol and CTAB micelles, as compared with an aqueous phosphate buffered medium, but with subtle differences in the visible region.

The time-dependent changes in the UV−vis spectrum of Fe(III)MP-8 upon oxidation by HOOH are depicted in Figure 2A. The inset shows the kinetics of the Soret band changes at 417 nm. The spectral changes observed during the peroxide-promoted oxidation of MP-8 bound to CTAB micelles (Fe(III)MP-8/CTAB), at pH 7.4, are similar to those observed by Primus et al.[13] during the reaction between Fe(III)MP-8 and HOOH, in carbonate buffer at pH 9.1, on a millisecond time

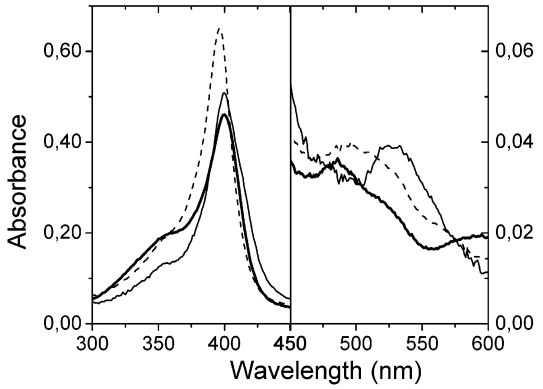

Figure 1. UV−vis spectra of 4 μM Fe(III)MP-8 in different media: 5 mM phosphate buffer, pH 7.4 (dashed line); 20 mM CTAB in phosphate buffer, pH 7.4 (thick solid line); and ethanol (thin solid line).

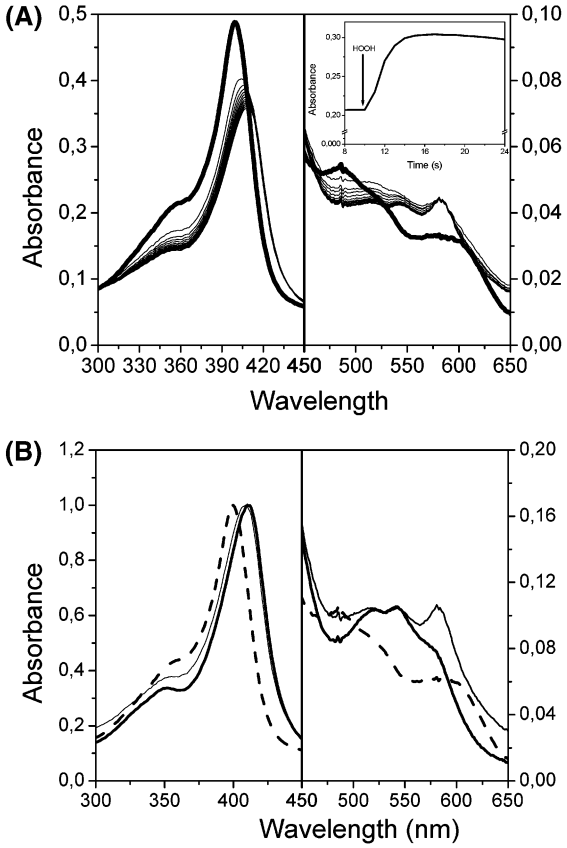

Figure 2. (A) Time-resolved UV−visible spectra of the reaction of 4.25 μM Fe(III)MP-8/CTAB with 0.8 mM HOOH at pH 7.4 (12 scans with an interval of 1 s). The inset shows the kinetics at 417 nm of the reaction of 4.25 μM Fe(III)MP-8/CTAB with 0.8 mM HOOH at pH 7.4. Typically 20 data points were acquired at $\lambda = 417$ nm. (B) UV−vis spectra of 4.25 μM Fe(III)MP-8 (dashed line) and the corresponding Compound II obtained during the reaction with 0.8 mM HOOH (thin solid line) and *t*-BuOOH (thick solid line). The spectra were normalized for clarity.

scale. Similar results were obtained when *t*-BuOOH was used as substrate (Figure 2B), except for the absence of the charge-transfer band at 581 nm which was substituted by a shoulder at the same wavelength. Surprisingly, the CTAB micellar microenvironment circumvented the necessity of employing rapid kinetics and allowed the same reaction to be accompanied on a scale of seconds. For both substrates, the spectral changes were compatible with the formation of Compound II, since in the presence of low peroxide concentrations (below 50 μM) the spectrum of MP-8/CTAB (not shown) obtained in the course

TABLE 1: Maximal Wavelength for the Different Species of MP-8 and MP-8/CTAB

MP-8 species	Soret band (nm)	Q-bands (nm)	CT band (nm)
Fe(III)MP-8	396	494	622
Fe(III)MP-8/CTAB	400	485 and 520	584
MP-8 Compound II	406	519 and 548	
MP-8 Compound II/CTAB	409	517 and 543	581[a]

[a] The CT (charge-transfer) band at 581 is substituted by a shoulder at the same wavelength, when Compound II is generated by *t*-BuOOH.

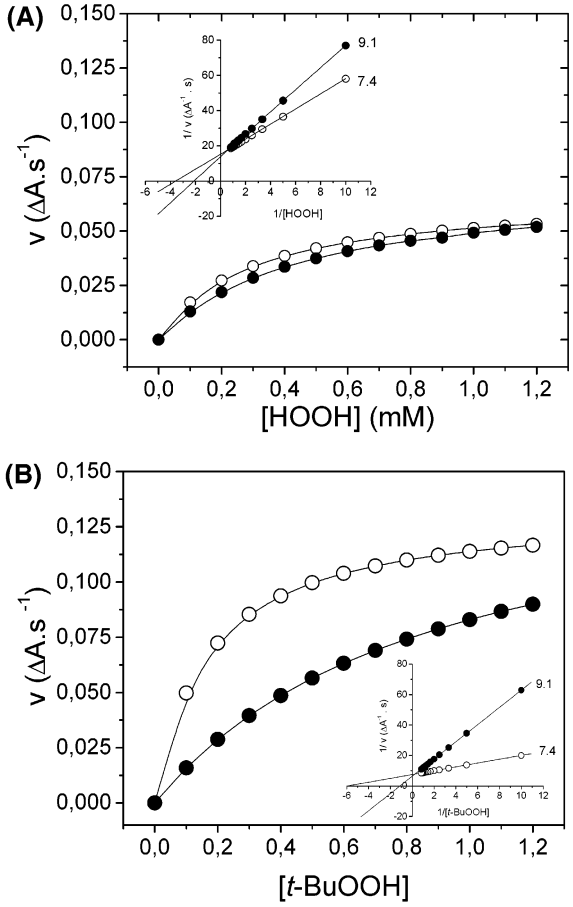

Figure 3. Variation of the rate of reaction for Fe(III)MP-8/CTAB and (A) HOOH or (B) *t*-BuOOH at pH 7.4 (open circles) and 9.1 (solid circles). The insets show the corresponding double-reciprocal plots for the data shown in (A) and (B). Error bars were omitted for clarity. The experiments were carried out with 4.25 μM Fe(III)MP-8 at 25 °C.

of the reaction exactly matches that obtained in the presence of a high concentration of peroxides (up to 1.2 mM), conditions under which Compound III could be formed. Compound III of peroxidases was first reported by Keilin and Mann[16] in the reaction of HRP with a large excess of HOOH and subsequently by many other researchers in the field of hemoprotein study,[4,17−20] but it has not been obtained in the presence of low hydrogen peroxide concentrations or in the presence of *t*-BuOOH. Furthermore, similar to that described for HRP,[21] Fe(III)MP-8/CTAB could be recovered from its Compound II form, obtained during the reaction with low peroxide concentrations (up to 50 μM), by the addition of 0.3 mM DPAA (diphenylacetaldehyde) (unpublished results). The maximal wavelength of the characteristic bands of native Fe(III)MP-8/CTAB and MP-8/CTAB Compound II are compared with those of the corresponding native Fe(III)MP-8 and MP-8 Compound II in buffered

TABLE 2: Kinetic Parameters for Reaction of Peroxide with Fe(III)MP-8

	pH 7.4			pH 9.1		
	K_m (mM)	k_2 (s^{-1})	k_2/K_m ($M^{-1}\cdot s^{-1}$)	K_m (mM)	k_2 (s^{-1})	k_2/K_m ($M^{-1}\cdot s^{-1}$)
t-BuOOH	0.17 ± 0.01	0.14 ± 0.01	808	0.9 ± 0.2	0.17 ± 0.02	189
HOOH	0.28 ± 0.03	0.066 ± 0.002	233	0.45 ± 0.04	0.069 ± 0.002	154
HOOH[a]	0.28	222	589 000	0.20	167	825 000

[a] According to data of ref 11 at pH 8.0.

aqueous medium (Table 1). Table 1 shows that, in CTAB micelles, the Fe(III)MP-8 and MP-8 Compound II spectra exhibited red-shifted Soret band peaks compared to those of Fe(III)MP-8 and MP-8 Compound II in aqueous medium, as expected for the heme group in a low-polarity microenvironment.[15]

The kinetic curves at the Soret band obtained for different pHs and [peroxide] for both substrates, HOOH and *t*-BuOOH, were analyzed using a exponential fit, ignoring the subsequent degradation steps of the catalyst. The rate of reaction for Fe(III)MP-8/CTAB at pH 7.4 and 9.1 was plotted as a function of [HOOH] and [*t*-BuOOH] and fitted to eq 2. The results are shown in panels A and B of Figure 3 for HOOH and *t*-BuOOH, respectively. The double-reciprocal plots of $1/v$ as a function of 1/[HOOH] and 1/[*t*-BuOOH] were linear (insets of Figure 3A and 3B, respectively). For both substrates, changing of the pH led to a significant difference in the Michaelis constant (K_m), but insignificant changes in the maximal rate (k_2). The results at pH 7.4 and 9.1 for the micellar system were opposite to those in aqueous medium.[13] In micelles, an increase of the slope was observed upon changing the pH from 7.4 to 9.1, indicating an increase in the K_m values. This effect was more drastic when *t*-BuOOH was used as substrate. Table 2 compares the kinetic constants obtained for the micellar system to literature data for HOOH determined in buffered aqueous medium. At pH 7.4, the K_m value for HOOH was 1.7 times higher than that for *t*-BuOOH. At pH 9.1, the result was inverted and K_m for *t*-BuOOH was 2 times higher than that for HOOH. When HOOH was the substrate, the pH change from 7.4 to 9.1 promoted a 1.6-fold increase in the K_m value (from 0.28 ± 0.03 to 0.45 ± 0.04 mM). However, for *t*-BuOOH, K_m increased 5.3-fold (from 0.17 ± 0.01 to 0.9 ± 0.2 mM) when the pH was increased from 7.4 to 9.1. On the other hand, in homogeneous medium, the Michaelis constant K_m was the same obtained for the micellar system in pH 7.4 (0.28 ± 0.2 mM) and was not significantly affected when the pH was increased from 7.4 to 9.1 (0.20 ± 0.3 mM).[13]

At this point it was necessary to consider the effect of pH on the cmc of CTAB. Under the same experimental conditions in which the kinetic experiments were performed, the cmc values obtained were 0.07 and 0.186 mM at pH 7.4 and 9.1, respectively. Below the cmc of CTAB, no spectral change was observed for Fe(III)MP-8 (not shown), but above the cmc of CTAB two spectrum types were observed for the heme peptide according to the CTAB micelle/Fe(III)MP-8 molar ratio (Figure 4). In a low CTAB micelle/Fe(III)MP-8 molar ratio (0.25), Fe(III)MP-8 exhibited a more drastic Soret band red shift as compared with the spectrum obtained in a significantly higher molar ratio (37), a condition where one MP-8 molecule per micelle was expected. In the visible region the difference between the spectra in the two different conditions was also evident (Figure 4). At a peroxide concentration of 0.8 mM, the rate of the reaction ($\Delta A\cdot s^{-1}$) for Fe(III)MP-8/CTAB, at the two pH values, 7.4 (inset Figure 4) and 9.1 (not shown), were plotted as a function of CTAB micelle/Fe(III)-MP-8 molar ratio over the range of 0.25−37 (above the cmc of CTAB). The results

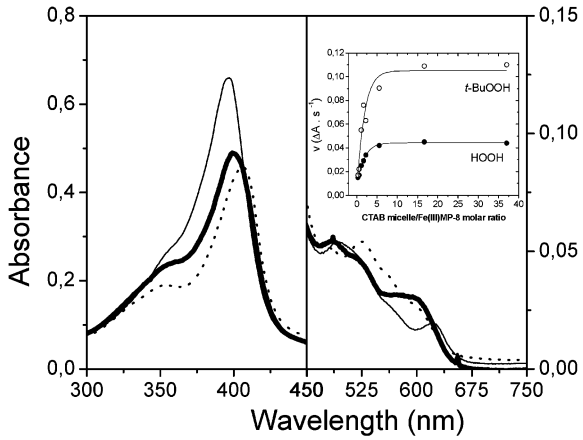

Figure 4. UV−vis spectra of 4.25 μM Fe(III)MP-8 in 5 mM phosphate buffered water (thin solid line), 0.15 mM CTAB (dashed line), and 20 mM CTAB (thick solid line). The inset shows the variation of the rate of reaction for Fe(III)MP-8/CTAB and 0.8 mM HOOH (solid circles) or *t*-BuOOH (open circles) at pH 7.4 as a function of the CTAB micelle/Fe(III)MP-8 molar ratio. The experiments were carried out at 25 °C.

showed no change in the rate values for either substrate over that range of CTAB micelle/Fe(III)MP-8 molar ratio where the CTAB micelles are occupied by only one MP-8 molecule, i.e., in molar ratios above 5 (inset Figure 4). Similar results were obtained at pH 9.1 (not shown).

In this system, two reaction mechanisms are possible for the peroxide cleavage: heterolytic cleavage generating peroxide reduced form (alcohol-derived for *t*-BuOOH and water for HOOH) and MP-8/CTAB Compound I (eq 6), or homolytic cleavage generating RO$^\bullet$ (*tert*-butyloxyl and hydroxyl radicals) and MP-8/CTAB Compound II (eq 7). In the heterolytic cleavage mechanism, Compound I could then attack another peroxide molecule generating peroxyl radical (eq 8), as depicted by Scheme 1.

Although there are a number of reactions by which RO$^\bullet$ radicals can be produced from ROO$^\bullet$ radicals and vice versa, the different mechanisms proposed in Scheme 1 dictate that the initial radical produced is either RO$^\bullet$ generated from the homolytic cleavage of peroxides, (eq 7) or ROO$^\bullet$ generated from the attack of Compound I on ROOH (eq 8). In this case, Compound I was formed by previous heterolytic cleavage of peroxides (eq 6). The reactions of the initial radical that occur after its production can be suppressed by increasing the concentration of a spin trapping such as DMPO, a method that was previously used by Ledwith et al.[22] and Barr and Mason.[11] According to this method, the more spin trap is added, the more initial radical is trapped. This prevents the initial radical from undergoing reactions with other species or itself that lead to secondary radicals. We used this strategy to determine whether the peroxyl or alkoxyl radical was the initial radical produced by the reaction of Fe(III)MP-8/CTAB with *t*-BuOOH. To do this, the relative contributions of the DMPO adducts were measured at various DMPO concentrations (Figure 5A). However, opposite to what occurred with cytochrome *c* catalyzed

SCHEME 1

$$\text{PorFe(III)-OH}_2 \rightleftharpoons \text{PorFe(III)-OH} + \text{H}^+ \quad (4)$$

$$\text{PorFe(III)-OH} + \text{ROOH} \rightleftharpoons \text{PorFe(III)-OOR} + \text{HOH} \quad (5)$$

$$\text{PorFe(III)-OOR} \longrightarrow \text{Por}^+\text{Fe(IV)=O} + \text{ROH} \quad \text{(heterolytic cleavage)} \quad (6)$$

$$\text{PorFe(III)-OOR} \longrightarrow \text{PorFe(IV)=O} + \text{RO}^\bullet \quad \text{(homolytic cleavage)} \quad (7)$$

$$\text{Por+Fe(IV)=O} + \text{ROOH} \longrightarrow \text{PorFe(IV)=O} + \text{ROO}^\bullet \quad (8)$$

cleavage of *t*-BuOOH, the peroxyl adduct was not detected and the first radical observed was adduct of a carbon-centered radical, probably CH_3**.** (Figure 5A, line a). This alkyl radical could be produced by the cleavage of *tert*-butyloxyl radical, according to eq 9.

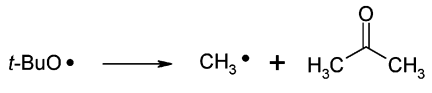

(9)

The relative contributions of the alkyl and alkoxyl adducts to the composite EPR spectrum were influenced by the concentration of DMPO (Figure 5A, lines a, b, and c, respectively). With the increase of DMPO concentration, the relative contribution of the alkyl radical adduct decreased, while that of the *tert*-butyloxyl radical increased. In these experiments, the relative concentrations of the radical adducts as represented by the low-field lines were calculated using computer simulation (Figure 5B,C). The EPR spectrum recorded from a reaction mixture containing Fe(III)MP-8/CTAB and *t*-BuOOH in the presence of 22 mM DMPO revealed a DMPO adduct (Figure 5B, line a) whose spectrum obtained by computer simulation (Figure 5B, line b) exhibited the hyperfine coupling constants $a^N = 16.00$ G and $a_\beta^H = 23.00$ G and could be assigned as alkyl (very similar to ref 11). In the presence of 360 mM of DMPO, the contribution of alkyl radical adduct disappeared (Figure 5C, line a). The simulation of the DMPO radical adduct (Figure 5C, line b) presented hyperfine coupling constants $a^N = 14.90$ G and $a_\beta^H = 15.80$ G and could be assigned as *tert*-butyloxyl. The same hyperfine coupling constants were obtained in the absence of CTAB: $a^N = 14.90$ G and $a_\beta^H = 15.80$ G (EPR spectrum and simulation not shown). The observed hyperfine parameters a^N and a_β^H for the cleavage of *t*-BuOOH by MP-8 in hetereogeneous and homogeneous media are close to the respective values presented in the literature for the same reaction catalyzed by cytochrome *c* in homogeneous medium[11] ($a^N = 14.90$ G and $a_\beta^H = 16.20$ G). The line width obtained in both media, when MP-8 was the catalyst, was slightly broader (0.86 G) than the literature data presented for cytochrome *c* (0.70 G). This difference could be due to the effect of ionic strength since the literature data were obtained in the presence of 100 mM phosphate buffer and, in our results, in 5 mM phosphate buffer (relative lower ionic strength). Splitting of γ-hydrogen ($a_\gamma^H = 0.68$ G) was detected for DMPO/*tert*-butyloxyl adduct in both homogeneous and micellar media.

The cleavage of HOOH by MP-8/CTAB in the presence of DMPO led to the appearance of a detectable EPR adduct signal only in the presence of high DMPO concentration (360 mM, not shown). This signal exhibited EPR parameter $a^N = 14.8$ G, $a_\beta^H = 15.3$ G, and line width = 1.2 G, which could be assigned to DMPO/$^\bullet$OH adduct[23] as expected for the homolytic cleavage of HOOH by MP-8/CTAB. In this system, another signal with $a^N = 14.8$ G, $a_\beta^H = 0.0$ G, and line width $a = 1.60$, $b = -0.15$, $c = 0.10$, including tumbling effect $a + bm + cm^2$ (EPR spectrum not shown) was also detected. These hyperfine parameters are compatible with DMPO adduct where the β-hydrogen was substituted by an organic ligand. The origin and identity of this signal remain to be elucidated. Interestingly, Barr and Mason[11] did not detect DMPO/hydroxyl adduct, but only DMPOx, during the reaction of HOOH and cytochrome *c* in phosphate buffer.

These results pointed to the homolytic cleavage of peroxides as the predominant mechanism for the activity of the lipoenzyme MP-8/CTAB. When the substrate used was *t*-BuOOH, although peroxyl radical has not been detected, alkyl radical was detected and could be produced by cleavage of *tert*-butyloxyl radical observed in the presence of high DMPO concentration. When the substrate was HOOH, the detection of DMPO/hydroxyl adduct corroborated that the homolytic cleavage also occurred for this substrate. In this case, the cleavage of hydroxyl radical could not occur but this radical could attack another HOOH molecule generating peroxyl radical and the detection of DMPO/peroxyl adduct, in lower DMPO concentrations, could be expected. However, probably due to the lower catalytic efficiency of MP-8/CTAB to catalyze HOOH cleavage, detectable EPR signals of DMPO adducts with HOOH-derived radicals were not detected in low DMPO concentrations (22 and 90 mM).

MP-8/CTAB heme iron EPR spectra were obtained in the course of the reaction with HOOH and *t*-BuOOH (panels A and B, respectively, of Figure 6), which also corroborated the proposed mechanism. In CTAB micelles, the Fe(III)MP-8/CTAB EPR spectrum (Figure 6A, line a) exhibited a signal at $g = 6.0$ typical of the high-spin form of MP-8 with pentacoordinated heme iron and axial symmetry. The large amount of MP-8 necessary for the EPR measurements led to the appearance of a small amount of the low-spin form of hexacoordinated MP-8. Three seconds after the addition of HOOH and 2 s after the addition of *t*-BuOOH, the EPR spectrum revealed a decrease in the Fe(III)MP-8 signal and the appearance of two very discrete signals with $g = 3.904$ and $g = 4.290$ with rhombic symmetry. The very low-intensity signal $g = 3.904$ can be attributed to MP-8 oxoferryl π-cation (MP-8 Compound I)[24,25] and the signal with $g = 4.290$ to the porphyrin ring chemically modified by free radicals. This high-spin species ($g = 4.290$) has been previously described during the reaction of cytochrome *c* with *t*-BuOOH[12] and with oxidized cardiolipin.[26] The intensity of these signals increased after 8 s of reaction with HOOH and after 10 s of reaction with *t*-BuOOH, with a concomitant decrease of the $g = 6.0$ signal. At subsequent times (above 1 min), $g = 6.0$ signal remained constant, the signal attributed to Compound I disappeared, and the signal at $g = 4.290$ increased (not shown), suggesting that this signal was produced by the consumption of an EPR silent compound, in this case, Compound II.[4] The very low intensity of the signal assigned to Compound I that required the heterolytic cleavage of the O−O bond indicated that the homolytic cleavage must be the principal route followed by the reaction. In this case, the

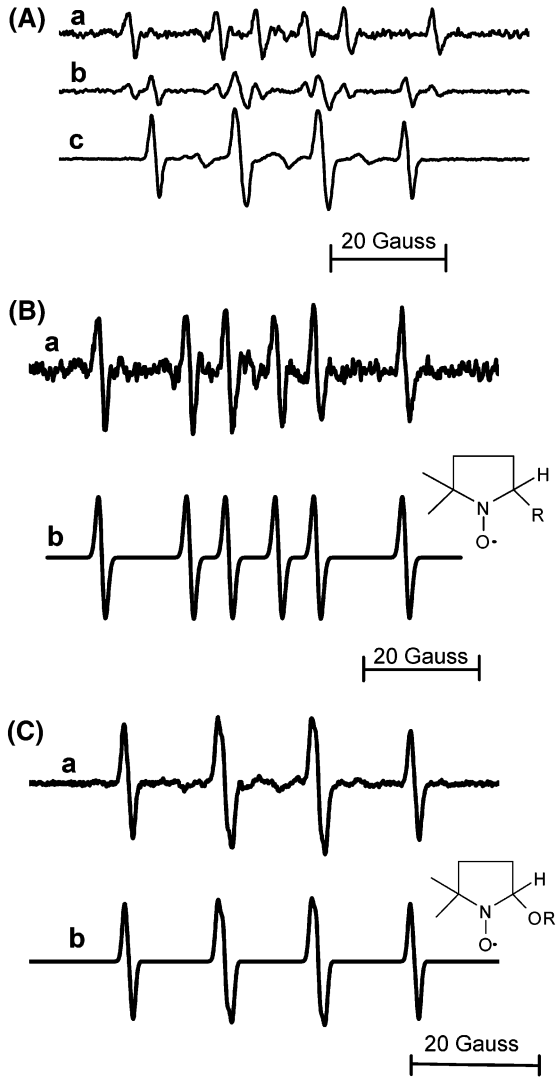

Figure 5. Experimental EPR spectra and computer simulation obtained from the reaction mixture containing Fe(III)MP-8/CTAB and *t*-BuOOH. (A) Line a corresponds to the experimental spectrum obtained using a mixture reaction containing 20 μM MP-8, 5.3 mM *t*-BuOOH, 20 mM CTAB, and 22 mM DMPO. Lines b and c correspond to the experimental spectra obtained under the same experimental conditions but in the presence of 90 and 360 mM DMPO, respectively. (B) Line a corresponds to the experimental spectrum obtained in the presence of 22 mM DMPO (same experimental conditions presented in panel A, line a), and line b is the individual simulation of the adduct signal in the spectrum a. The simulated spectra exhibited the hyperfine coupling constants $a^{N} = 16.0$ G and $a_{\beta}^{H} = 23.0$ G, with a_{γ}^{H} not observed for spectrum b. In this panel, line b is the simulated spectrum for DMPO/R(alkyl): line width 1.30 G and Gaussian line shape. (C) Line a corresponds to the experimental spectrum obtained in the presence of 360 mM DMPO (same experimental conditions presented in panel A, line c), and line b is the individual simulation of the adduct signal in spectrum a. The simulated spectra exhibited the hyperfine coupling constants $a^{N} = 14.90$ G, $a_{\beta}^{H} = 15.80$ G, and $a_{\gamma}^{H} = 0.68$ G for spectrum b. In this panel, line b is the simulated spectrum for DMPO/OR(*tert*-butyloxyl): line width 0.86 G and Gaussian line shape. Spectrometer conditions: modulation amplitude 0.05 mT, microwave power 20 mW, room temperature, scan time 2 min, scan range 100 G, receiver gain 1.6×10^4.

very low yield of peroxyl radical could explain the absence of a signal from peroxyl radical adduct.

Discussion

Reaction Mechanism in CTAB Micelles. This work describes the kinetics of formation of MP-8 Compound II upon reaction with peroxides in the presence of CTAB micelles as a function of substrate type (HOOH or *t*-BuOOH), pH, and CTAB concentration. For both substrates, the saturation kinetics (Figure 3) strongly suggested that the reaction follows the same pathway in the presence and absence of micelles.[13] Primus et al.,[13] on the basis of the detection of EPR signal from manganese substituted MP-8 Compound II, have proposed heterolytic cleavage as the mechanism for oxidation of Fe(III)MP-8 by HOOH in homogeneous medium. However, detection of Compound II is not evidence of heterolytic cleavage since, as shown in Scheme 1, Compound II could be formed in both mechanisms, homolytic and heterolytic cleavage. Our results with DMPO spin trapping, in the presence (Figure 5) and absence of CTAB (EPR spectra not shown), pointed to the homolytic cleavage of peroxides as the predominant catalytic pathway for the oxidation of MP-8 by peroxides. Scheme 2 shows the proposed reaction mechanism, considering that all MP-8 molecules associated to CTAB micelles are coordinated with deprotonated water and D is the MP-8 form that exhibits Soret band bleaching.

Scheme 2 depicts a comparison between the reaction of Fe(III)MP-8 in aqueous and in micellar media that is in accordance with eqs 2 and 3 (see Experimental Section), since k_{obs} in aqueous medium encompasses also K_a, the PrFe(III)-OH_2 deprotonation step.

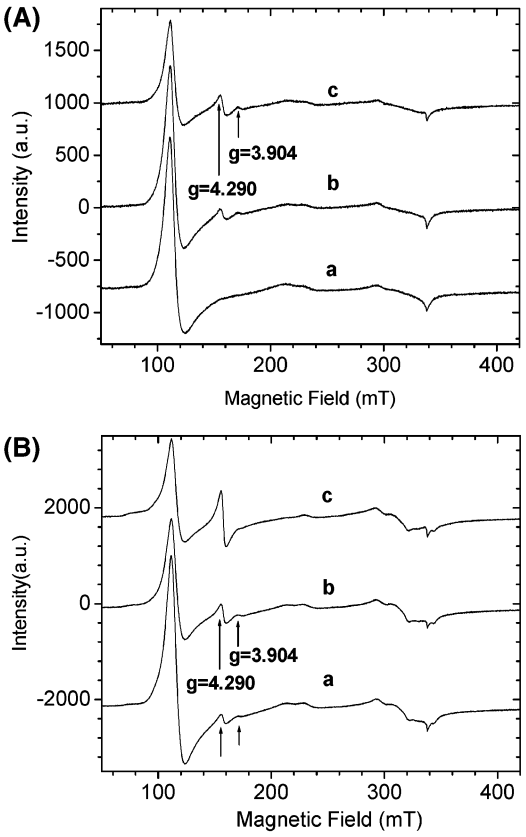

Figure 6. (A) Direct EPR analysis of 100 μM MP-8/CTAB species obtained in the course of the reaction with HOOH at (a) 0, (b) 3, and (c) 8 s in the presence of 60 mM CTAB in 5 mM phosphate buffer, pH 7.4, at 25 °C. The spectra were obtained at 11 K and frequency 9.4840 61 GHz. (B) Direct EPR analysis of 100 μM MP-8/CTAB species obtained in the course of the reaction with *t*-BuOOH at (a) 1, (b) 2, and (c) 10 s in the presence of 60 mM CTAB in 5 mM phosphate buffer, pH 7.4, at 25 °C. The spectra were obtained at 3.7 K and frequency 9.4855 01 GHz. Spectrometer conditions: gain 5×10^3, modulation amplitude 1.0 mT, microwave power 4 mW, time constant 10.24 ms, and conversion time 81.92 ms.

SCHEME 2

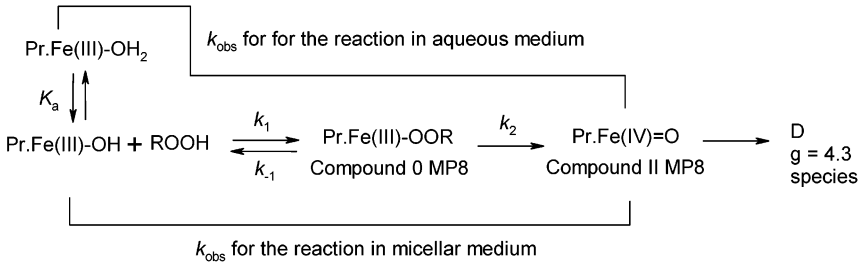

For the reaction occurring in the micellar system

$$1 + \frac{[H+]}{K_a} = 1 \tag{10}$$

since all Fe(III)MP-8 molecules were localized into the micelles and therefore

$$K_{m,app} = \frac{k_{-1} + k_2}{k_1} = K_m \tag{11}$$

In homogeneous medium,[13] linear fits of $1/k_{obs}$ at different pH values exhibited a different slope and a common intercept on the vertical axis, indicating that protons played a competitive role in the formation of Compound 0 and subsequent forms of oxidized MP-8. The effect of protons was further confirmed by the results of k_{obs} as a function of the proton concentration for a specific hydrogen peroxide concentration. Our analysis of the Supporting Information provided by Primus et al.[13] pointed to no significant alteration in the K_m value (Table 2) upon decreasing the pH from 9.1 to 8.0. In the presence of CTAB micelles, different results were obtained for both substrates when the medium pH value was decreased from 9.1 to 7.4 (Table 2); i.e., the K_m for both substrates decreased with the pH. The change of the K_m(HOOH)/K_m(*t*-BuOOH) ratio from 1.6 to 0.5 at pH 7.4 and 9.1, respectively, suggested that at high pH (above 9.1) both peroxides have similar partition coefficients in CTAB micelles. Under this condition (pH $\geq$9.1 in the bulk phase), the higher pH values found at the CTAB micellar interface (around 11.0) might lead to the ionization of *t*-BuOOH and HOOH molecules and loss of the affinity to the micelle core. At lower pH values (below 9.1), however, protonated HOOH, being more polar than *t*-BuOOH, remained partitioned preferentially into the water while nonionized *t*-BuOOH gained affinity to the micelle core. This is in accordance with literature data[27] revealing that, at pure water pH value, *t*-BuOOH was 40% incorporated into the micellar pseudophase of CTAC micelles, while HOOH was 15% under the same conditions. In this regard, at pH 7.4, the k_2 for the reaction with *t*-BuOOH was 2 times higher than for HOOH (Table 2).

Several researchers in the field of hemoprotein study[4,16−20] have been studying oxidized intermediates of peroxidases. All peroxidases studied so far share much of the same catalytic cycle consisting of three distinct and essentially irreversible steps[28] that form the cycle of peroxidases. The resting ferric enzyme binds reversibly the substrate, HOOH, forms the complex known as Compound 0, and reacts with the substrate in a two electron process to generate the intermediate known as Compound I. Compound I can carry out a single electron reduction of a substrate to generate Compound II. In this regard, certain peroxidases, such as HRP[27] and even MP-8 Compound I,[6] can utilize HOOH to reduce Compound I when no other substrate is available (Scheme 1, eq 8). Reaction of Compound II with more HOOH yields Compound III, a complex between ferric peroxidase and superoxide ion, known as oxyperoxidase. However, Compound 0 can also directly lead to Compound II, after homolytic cleavage of the O−O bond (Scheme 1, eq 7). According to the results showed in Figures 5 and 6, the homolytic scission of the O−O bond leading to the formation of MP-8/CTAB Compound II and a^N radical seems to be the predominant route and the rate-determining step of the reaction. The a^N radical would then lead to a chain-radical destruction of the heme and the appearance of a signal for a rhombic iron(III) species characterized by a signal at $g = 4.290$. The formation of the $g = 4.290$ signal coming from an EPR silent species, attributed here to Compound II, is also good evidence for the proposed mechanism. This mechanism has been described for the reaction of *t*-BuOOH with cytochrome *c*.[11,12]

The heterolytic cleavage of the O−O bond with the generation of MP-8CTAB π-cation oxoferryl species can hardly be the case in this system under the experimental conditions used here, i.e., at basic pH provided by the positively charged interface. In peroxidases, this is favored by the protonation of the second oxygen atom of the peroxide assisted by a distal histidine residue. Surprisingly, Wang et al.[6] have detected the formation of MP-8 Compound I in the presence of potassium phosphate buffer, pH 9.1. However, in the presence of CTAB micelles, the very low intensity of the MP-8CTAB π-cation oxoferryl signal detected for both substrates corroborates that the heterolytic cleavage of peroxides is not the preferential reaction mechanism adopted by the lipoenzyme MP-8/CTAB.

The present results point to k_2 as the rate constant for one nonreversible elementary step, the homolytic cleavage of the O−O bond of peroxides (Scheme 2).

Enzymatic Model. In the presence of CTAB micelles, substrate deprotonation plays a competitive role in the reaction, as attested to by the results obtained at pH 9.1. At the alkaline pH values, it is particularly interesting to compare the two substrates, HOOH and *t*-BuOOH. For both substrates in CTAB micelles, an increase of the pH led to an increase in the K_m values, but for HOOH the K_m value increased 1.6-fold while for *t*-BuOOH the K_m value increased 5.3-fold. At this point, it is important to consider the structure of the catalyst. MP-8 has a net negative charge due to its heme propionate groups and the carboxy group of the C-terminal oligopeptide chain, providing electrostatic affinity for the cationic CTAB micelle surface. However, the hydrophobic groups present in the oligopeptide chain with the also hydrophobic heme group must exhibit affinity for the micelle core. Hence, we propose a model for MP-8 associated with CTAB, where the heme propionate groups are associated to the micelle surface and the porphyrin ring and oligopeptide chain side is partially inserted into the micelle (Scheme 3).

This model is in accordance with the spectral changes observed when MP-8 is bound to CTAB micelles (Figure 1). The bathochromic effect observed for the Soret band is typical

SCHEME 3

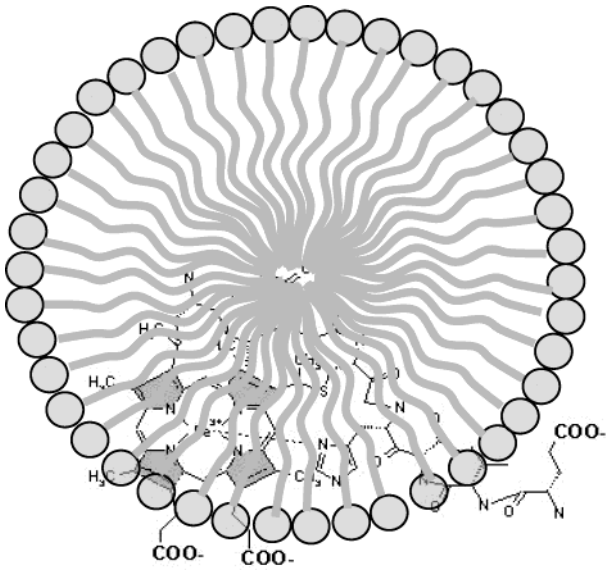

of the heme group in a hydrophobic microenviroment.[15] In this model, the micelle constitutes an artificial enzymatic active site for which hydrophobic substrates will exhibit higher affinity. This is in accordance with the lower K_m value obtained for *t*-BuOOH (0.17 ± 0.01 mM), which is the more hydrophobic substrate compared with HOOH (0.28 ± 0.03 mM), at pH 7.4. Therefore, the partitioning of substrates into the micelles, influenced by the interfacial pH, is a significant factor in determining the K_m. In homogeneous medium,[13] the K_m values at pH 8.0 and 9.1 were similar and matched the value obtained in CTAB micelles at pH 7.4 (Table 2), reinforcing the proposal of HOOH partitioned preferentially in the water phase. When the pH of the bulk phase is 7.4, CTAB micelles provide a microenvironment where the local pH is significantly higher than in the bulk, favoring the heme iron bound water deprotonation (see Scheme 2). When the bulk pH is 9.1, the local pH at the micelle surface is certainly higher, perhaps enough to promote deprotonation of peroxides, impairing their access to the "enzyme" active site (micelle interior) and decreasing their affinity for the "enzyme active site". This proposal is consistent with the increase of K_m for both substrates at pH 9.1. In agreement with this model, the more significant effect of pH observed for *t*-BuOOH can be attributed to differences in the partitioning of the substrate molecules in this heterogeneous medium.

In this model of catalyst the CTAB micelle/Fe(III)MP-8 molar ratio is another important factor in determining the efficiency of the reaction (Figure 4). Figure 4 suggests that, in low CTAB micelle/Fe(III)MP-8 molar ratios (below 5), Fe(III)MP-8 and CTAB micelles might form aggregates with probably two Fe(III)MP-8 molecules associated to the one micelle. Under this condition, the spectral changes (red shift of the Soret band and decreasing 1.4-fold in ϵ value) are in accordance with previous results obtained with Fe(III)MP-11 in high concentration (18.9 μM) in aqueous medium.[29] In the case of Fe(III)MP-8 dimers in CTAB micelles, the spectral alterations are thought to occur by intermolecular coordination of the metal by the N-terminal group at Cys14 which has been previously deprotonated in the alkaline microenviroment of the micellar interface. In high CTAB micelle/Fe(III)MP-8 molar ratios (above 5) the monomer forms of Fe(III)MP-8 associated to CTAB micelles are favored and the system exhibits the catalytic properties described in this work (inset Figure 4).

Catalytic Efficiency. A question arises upon comparison of the k_2/K_m values shown in Table 2: Why does the enzyme constructed via the association of MP-8 with CTAB micelles exhibit so low a catalytic efficiency? According to Primus et al.,[13] His42 could be responsible for the heme iron bound water deprotonation in HRP. Recent literature data[13] suggest that His42 acts initially as a proton acceptor (base catalyst) and then as a donor (acid catalyst) at neutral pH, consistent with the observed slower rate and lower efficiency of heterolytic cleavage observed at acid pH. Arg38 is influential in lowering the pK_a of His42, as well as in aligning HOOH in the active site, but it does not play a direct role in proton transfer. The role of distal Arg was also demonstrated in the reaction of Fe(III)MP-8 with HOOH in aqueous medium. In that case, the peroxidase activity of MP-8 was increased more than 10-fold by the presence of the guanidinium ion able to form the ion pair $GuaH^+HO_2^-$.[30] In homogeneous medium, exposure of the oxoferryl to the medium could facilitate the access to proton donors, such as water and neighboring amino acid groups of MP-8. For the enzyme MP-8/CTAB, the formation of the hydroperoxo species in the micellar enzymatic active site impairs the access to proton donors, slowing the catalytic process. It is noticeable that, in both homogeneous and micellar medium, the different catalytic efficiencies observed at the different pH values are due to the differences between the K_m values.

Conclusions

This is a novel work showing that the association of MP-8 with CTAB micelles produces a complex that can act as a lipoenzyme with specificity for different substrates and is able to form the same peroxidase intermediates, including Compound II. The most interesting characteristic of this enzyme is that the active site is a pocket formed not by a structured polypeptide chain, but by a detergent aggregate. This aggregate provides the hydrophobic microenvironment commonly found in peroxidases. On the basis of these results, we intend to realize further studies to better characterize and improve this catalytic complex.

Acknowledgment. We are grateful to the Fundação de Amparo à Pesquisa do Estado de São Paulo (FAPESP) and the CNPq for financial support and to Prof. Dr. Frank H. Quina for a critical reading of the manuscript. A first account of these results was presented as a poster in the XXXII Annual Meeting of the Brazilian Society of Biochemistry and Molecular Biology (SBBq).

References and Notes

(1) Aron, J.; Baldwin, D. A.; Marques, H. M.; Pratt, J. M.; Adams, P. A. *J. Inorg. Biochem.* **1986**, *27*, 227−243.
(2) Wang, J. S.; Vanwart, H. E. *J. Phys. Chem.* **1989**, *93*, 7925−7931.
(3) Munro, O. Q.; Marques, H. M. *Inorg. Chem.* **1996**, *35*, 3752−3767.
(4) Dunford, H. B.; Stillman, J. S. *Coord. Chem. Rev.* **1975**, *19*, 187−251.
(5) Baek, H. K.; Van Wart, H. E. *Biochemistry* **1989**, *28*, 5714−5719.
(6) Wang, J. S.; Haesun, K. B.; Van Wart, H. E. *Biochem. Biophys. Res. Commun.* **1991**, *179*, 1320−1324.
(7) Mukai, M.; Nagano, S.; Tanaka, M.; Ishimori, K.; Morishima, I.; Ogura, T.; Watanabe, Y.; Kitagawa, T. *J. Am. Chem. Soc.* **1997**, *119*, 1758−1766.
(8) Ortiz de Montellano, P. R. *Annu. Rev. Pharmacol. Toxicol.* **1992**, *32*, 89−107.
(9) Savenkova, M. I.; Kuo, J. M.; Ortiz de Montellano, P. R. *Biochemistry* **1998**, *37*, 10828−10836.
(10) Smith, A. T.; Veitch, N. *Curr. Opin. Chem. Biol.* **1998**, *2*, 269−278.
(11) Barr, D.; Mason, R. P. *J. Biol. Chem.* **1995**, *270*, 12709−12716.

(12) Nantes, I. L.; Alário, A. F.; Nascimento, O. R.; Bandy, B.; Gatti, R.; Bechara, E. J. H. *Free Radical Biol. Med.* **2000**, *28*, 786−796.
(13) Primus, J. L.; Grunenwald, S.; Hagedoorn, P. L.; Albrecht-Gary, A.-M.; Mandon, D.; Veeger, C. *J. Am. Chem. Soc.* **2002**, *124*, 1214−1221.
(14) Nelson, D. P.; Kiesow, L. A. *Anal. Biochem.* **1972**, *49*, 474−478.
(15) Makarska, M.; Radzki, St.; Legendziewicz, J. *J. Alloys Compd.* **2002**, *341*, 233−238.
(16) Keilin, D.; Mann, T. *Proc. R. Soc. London, B* **1937**, *122*, 119−133.
(17) Chance, B. *Arch. Biochem. Biophys.* **1952**, *41*, 404−415.
(18) Dunford, H. B. *Heme Peroxidases*; Wiley-VCH: New York, 1999; pp 281−308.
(19) Nakajima, R.; Yamasaki, I. *J. Biol. Chem.* **1987**, *262*, 2576−2581.
(20) Hiner, N. P. A.; Ruiz, J. H.; López, J. N. R.; Cánovas, F. G.; Brisset, N. C.; Smith, A. T.; Arnao, M. B.; Acosta, M. *J. Biol. Chem.* **2002**, *277*, 26879−26885.
(21) Nantes, I. L.; Bechara, E. J. H.; Cilento, G. *Photochem. Photobiol.* **1996**, *63*, 702−708.
(22) Ledwith, A.; Russell, P. J.; Sutcliffe, L. H. *Proc. R. Soc. London, A* **1973**, *332*, 151−166.
(23) Singh, R. J.; Karqui, H.; Gunther, M. R.; Beckman, J. S.; Mason, R. P.; Kalyanaraman, B. *Proc. Natl. Acad. Sci. U.S.A.* **1998**, *95*, 6675−6680.
(24) Assis, M. D.; Serra, O. A.; Iamamoto, Y.; Nascimento, O. R. *Inorg. Chim. Acta* **1991**, *187*, 107−114.
(25) Khindaria, A.; Aust, S. D. *Biochemistry* **1996**, *35*, 13107−131111.
(26) Zucchi, M. R.; Nascimento, O. R.; Faljoni, A. A.; Prieto, T.; Nantes, I. L. *Biochem. J.* **2003**, *370*, 671−678.
(27) Encinas, M. V.; Lissi, E. A. *Photochem. Photobiol.* **1983**, *37*, 251−255.
(28) Dunford, H. B. In *Peroxidases in Chemistry and Biology*; Everse, J., Everse, K. E., Grisham, M. B., Eds.; CRC Press: Boca Raton, FL, 1991; pp 1−24.
(29) Marques, H. M.; Perry, C. B. *Inorg. Biochem.* **1999**, *75*, 281−291.
(30) Baldwin, D. A.; Marques, H. M.; Pratt, J. M. *J. Inorg. Biochem.* **1987**, *30*, 203−217.